Effect of electrical double layer on electric conductivity and pressure drop in a pressure-driven microchannel flow

Heng Ban, Bochuan Lin, and Zhuorui Song

Effect of electrical double layer on electric conductivity and pressure drop in a pressure-driven microchannel flow

Heng Ban, Bochuan Lin, and Zhuorui Song
*Department of Mechanical and Aerospace Engineering, Utah State University,
Logan, Utah 84322, USA*

The effect of an electrical double layer (EDL) on microchannel flow has been studied widely, and a constant bulk electric conductivity is often used in calculations of flow rate or pressure drop. In our experimental study of pressure-driven micropipette flows, the pipette diameter is on the same order of magnitude as the Debye length. The overlapping EDL resulted in a much higher electric conductivity, lower streaming potential, and lower electroviscous effect. To elucidate the effect of overlapping EDL, this paper developed a simple model for water flow without salts or dissolved gases (such as CO_2) inside a two-dimensional microchannel. The governing equations for the flow, the Poisson, and Nernst equations for the electric potential and ion concentrations and the charge continuity equation were solved. The effects of overlapping EDL on the electric conductivity, velocity distribution, and overall pressure drop in the microchannel were quantified. The results showed that the average electric conductivity of electrolyte inside the channel increased significantly as the EDL overlaps. With the modified mean electric conductivity, the pressure drop for the pressure-driven flow was smaller than that without the influence of the EDL on conductivity. The results of this study provide a physical explanation for the observed decrease in electroviscous effect for microchannels when the EDL layers from opposing walls overlap. © *2010 American Institute of Physics.* [doi:10.1063/1.3328091]

I. INTRODUCTION

When water flows through a microchannel or tube, a glass pipette, for instance, the charge on the wall surface (glass) leads to the formation of an electrical double layer (EDL) next to the wall. The counterion concentration inside the EDL affects the flow behavior inside the channel. The influence of the EDL on microchannel flow has been studied widely.[1–7] Most researches have focused on the microchannel flow with the width of the channel ten times greater than Debye length $(1/\kappa)$, which is a characteristic thickness for the EDL. Here, κ is the Debye–Huckel parameter. Under such a condition, the electric potential distribution for a plate with fluid occupying a semi-infinite space can often be used to describe the potential distribution across the channel. When the channel width is much larger than the EDL thickness, the Poisson–Boltzmann equation can be solved with the boundary condition at the middle plane between the two channel walls where the electric potential is zero and the ionic concentrations are equal to the original bulk ionic concentrations. Furthermore, the Debye–Huckel approximation can simplify the Poisson–Boltzmann equation and result in a simple analytic solution of potential across the channel.[7] However, the Debye–Huckel theory is only suitable for cases with small zeta potential or large distance between walls, specifically, under the condition of $|\beta|=|ze\zeta/k_bT| \ll 1$, where k_b is the Boltzmann constant, T is temperature, z is valence, e is the charge of an electron, ζ is the zeta potential of the wall, and β is the property ratio. For the case of $|\beta|>1$, the nonlinear Poisson–Boltzmann equation needs to be solved for the potential distribution.[2,6] In most cases, the solution for the Poisson–Boltzmann equation in semi-infinite domain is sufficient to describe the potential distribution because the EDL thickness is usually much smaller than the channel width. For cases

of narrow channels with overlapped EDL, previous studies have largely overlooked the change in electric conductivity of the electrolyte, and a number of papers over the past 10 years have chosen a constant electric conductivity, independent of the EDL, when applying the zero total current condition.[8,9] This is despite Hunter's[1] clarity that it is unacceptable because the conductivity depends on the ion concentration distribution and despite the fact that analytical solutions for uniform channels have been available for decades.[10–12] For instance, Li developed an analytic solution but then failed to use that solution for calculating EDL conductivity by choosing the conductivity independently.[8] Chun and Kwak gave a related more recent analysis for slit flow but also ignored the EDL conductivity when they could have used their solution to calculate it.[9] The influence of overlapping EDL on pressure-driven flows needs to be further investigated with detailed examination of electric conductivity of the electrolyte in order to establish a better understanding of the effect of overlapping EDL on electric conductivity.

For pressure-driven flows, the effect of EDL on the flow arises through the emergence of the electric field along the flow direction, often measured as the streaming potential. The streaming potential is established by the accumulation of counterions downstream to create a conduction current, which is in balance with the streaming current caused by the electrolyte transport due to the bulk flow.[13,14] The streaming current is proportional to the streaming potential and the fluid conductivity. In most previous research,[7,15] a constant value of electric conductivity independent of the EDL is used, although the value widely varies. Fundamentally, the electric conductivity of an electrolyte is a function of types of ions and ion concentrations.[13] Inside the EDL, the redistribution of ions due to the appearance of charges on surfaces leads to the variation in the electric conductivity. Once the channel size decreases to make the EDL from opposite walls overlap, the overall variation in the electric conductivity across the channel becomes significant. Therefore, it is unacceptable to treat the electric conductivity as a constant independent of channel size. The value of the electric conductivity has to be established based on the local ion distributions.

Either the zeta potential or the surface charge density on the wall is needed in order to solve the Poisson equation for the electric potential distribution across the channel. For instance, if the surface change density is specified, the ion concentrations can be completely determined, and the electric potential distribution can also be determined within a constant.[16,17] To completely specify the potential, a reference point is needed with a given value of the potential at a specific location. The zeta potential at the wall is a reference point frequently used. Another way is to specify the potential at the center of the channel. Some researchers[7,18] suggest using the site-dissociation model by Healy and White[19] to calculate the surface charge density. In that model, the calculation of surface charge density depends not only on the zeta potential but also on the pH value of the water at the point of zero net charge, pHz. The surface charge density at the wall is related to the zeta potential, and it can be calculated directly from the zeta potential and the properties of the electrolyte.[20]

In this paper, an analytic model was established for pressure-driven flows with strong overlapped EDL in micro- or nanochannels as an initial effort to study the electric conductivity effect on electroviscous effect. The model accounted for the variation in local electric conductivity for pure water without salts or dissolved gases such as CO_2. With the modified electric conductivity, the predicted streaming potential and overall electroviscous effect were smaller than those without considering the effect of overlapping EDL on electric conductivity. The potential distribution across the channel was obtained with overlapping EDL effect, and the comparison with models without EDL overlapping showed that the current model is closer to the exact solution than the traditional model using the solution of Poisson–Boltzmann equation for the semi-infinite domain.

II. THEORY AND ANALYSIS

For fully developed fluid flow between two infinitely large parallel plates, schematically shown in Fig. 1, the EDL and fluid flow are considered one-dimensional. The fluid inside the microchannel was de-ionized ultrafiltered (DIUF) water, which can be considered as a 1:1 symmetric electrolyte solution. In order to investigate the influences of the EDL on the flow inside the
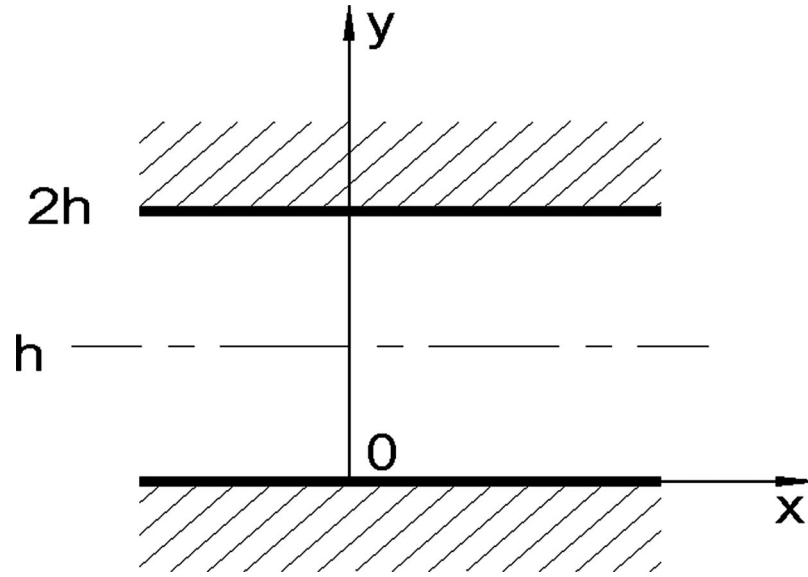
FIG. 1. Coordinates of parallel microchannel and half channel width is h.

microchannel, the Poisson and Nernst equations for potential and ion distributions and the Navier–Stokes equation for flow are solved by considering electrolyte solution electric conductivity changes due to ion distribution.

A. Analytic solution for potential and charge distributions

The electric potential ψ inside the channel is dependent on the net charge density ρ_e, and it is governed by the Poisson equation,

$$\frac{d^2\psi}{dy^2} = -\frac{\rho_e}{\varepsilon},$$ (1)

where ε is the permittivity of fluid. The boundary conditions at the channel wall include the zeta potential ζ at the wall surface, which has a charge density σ_w,

$$\psi = \zeta \quad \text{at} \quad y = 0,$$ (2)

and the symmetric condition at the center of the channel,

$$\frac{d\psi}{dy} = 0 \quad \text{at} \quad y = h.$$ (3)

The net charge density ρ_e can be expressed with local ionic concentrations for cation and anion, n_+ and n_-,

$$\rho_e = ze(n_+ - n_-).$$ (4)

Equation (4) is suitable for the symmetric electrolyte solutions, and z is the absolute value of the valence of electrolytes. The relationship between the ionic concentration and the electric potential is described by the Nernst equation,

$$\frac{1}{n_\pm} = \frac{dn_\pm}{dy} = \mp \frac{ze}{k_bT}\frac{d\psi}{dy}.$$ (5)

Defining ion concentrations at the channel center with subscript h,

$$n_+ = n_{+h}, \quad n_- = n_{-h}, \quad \psi = \psi_h \quad \text{at} \quad y = h, \tag{6}$$

the Nernst equation can be solved for ionic concentrations in the channel,

$$n_\pm = n_{\pm h} e^{\mp (ze/k_b T)(\psi - \psi_h)}. \tag{7}$$

The ionic concentration is assumed to obey the equilibrium condition

$$n_+ \cdot n_- = n_0^2, \tag{8}$$

where n_0^2 denotes equilibrium concentration. The net charge density in Eq. (4) can be determined based on the solution of the Nernst equation, given by Eq. (7), and the equilibrium condition for ions, given by Eq. (8). In order to normalize the Poisson equation, we define dimensionless potential, dimensionless length, and dimensionless ionic concentration as

$$\Phi = \psi / \zeta, \tag{9}$$

$$Y = y/h, \tag{10}$$

$$\bar{n}_\pm = n_\pm / n_0 \tag{11}$$

and further define two dimensionless parameters,

$$\kappa = \left(\frac{2 n_0 z^2 e^2}{\varepsilon k_b T} \right)^{1/2}, \tag{12}$$

$$\beta = \frac{ze\zeta}{k_b T}. \tag{13}$$

The Poisson equation can be expressed in a dimensionless form,

$$\frac{d^2 \Phi}{dY^2} = - \frac{\kappa^2 h^2}{2\beta} (\bar{n}_{+h} e^{-\beta(\Phi - \Phi_h)} - \bar{n}_{-h} e^{\beta(\Phi - \Phi_h)}). \tag{14}$$

The boundary conditions also become

$$\Phi = 1 \quad \text{at} \quad Y = 0, \tag{15}$$

$$\frac{d\Phi}{dY} = 0, \quad \text{at} \quad Y = 1. \tag{16}$$

As the channel height decreases to as small as Debye length, coion concentrations are much lower than those of counter ions, similar to the case of ion concentrations inside the EDL layers. A common treatment for ion concentrations inside the EDL layer is to assume that the contribution by coions to the electric field is negligible compared to that by counterions. For cases of $\zeta < 0$ (i.e., the surface charge is negative), we have $\beta < 0$, and the concentration of cation is much larger than that of anion, $\bar{n}_+ \gg \bar{n}_-$. Therefore, we have

$$\bar{n}_{+h} e^{-\beta(\Phi - \Phi_h)} \gg \bar{n}_{-h} e^{\beta(\Phi - \Phi_h)}, \tag{17}$$

which indicates that the right side can be neglected in calculation. After omitting $\bar{n}_{-h} e^{\beta(\Phi - \Phi_h)}$, the dimensionless Poisson equation, Eq. (14), can be rewritten as

$$\frac{d^2\Phi}{dY^2} = -\frac{\kappa^2 h^2}{2\beta}\bar{n}_{+h}e^{-\beta(\Phi-\Phi_h)} \quad (\zeta < 0, \beta < 0). \tag{18}$$

Similarly, for $\zeta > 0$, $\bar{n}_+ \ll \bar{n}_-$, the Poisson equation can be simplified,

$$\frac{d^2\Phi}{dY^2} = \frac{\kappa^2 h^2}{2\beta}\bar{n}_{-h}e^{\beta(\Phi-\Phi_h)} \quad (\zeta > 0, \beta > 0). \tag{19}$$

The above two equations can be combined into one expression to account for the signs of β,

$$\frac{d^2\Phi}{dY^2} = \frac{\kappa^2 h^2}{2|\beta|}n_h e^{|\beta|(\Phi-\Phi_h)}, \tag{20}$$

where $n_h = \max(\bar{n}_{+h}, \bar{n}_{-h})$, which is the dimensionless concentration of counterions at the channel center. Using the symmetric condition at the center of the channel, $d\Phi/dY = 0$, $\Phi = \Phi_h$, at $Y = 1$, Eq. (20) can be solved for $d\Phi/dY$, and the solution can be written as

$$\left(\frac{d\Phi}{dY}\right)^2 = \frac{\kappa^2 h^2}{\beta^2}n_h(e^{|\beta|(\Phi-\Phi_h)} - 1). \tag{21}$$

The solution of Eq. (21) is given by

$$\Phi = -\frac{2}{|\beta|}\ln\{\cos[\Omega(1-Y)]\} + \Phi_h, \tag{22}$$

where $\Omega = \kappa h \sqrt{n_h}/2$. This expression of potential distribution contains two parameters to be determined: the ionic concentration n_h and the potential Φ_h at the center of the channel. These two parameters are introduced as boundary conditions to confine the Nernst equation, Eq. (5), and are needed to be determined by other constraints. n_h can be determined from the electric neutral condition across the channel when the channel is sufficiently long. At any cross-section, the net charge of the electrolyte inside the channel is equal to the net natural surface charge on the channel wall, σ_w,

$$-\sigma_w = \int_0^h \rho_e dy. \tag{23}$$

Combining Eq. (1) and Eq. (23), the gradient of the potential at the wall can be determined by the surface charge density, σ_w,

$$\frac{d\psi}{dy}\bigg|_{y=0} = -\frac{\sigma_w}{\varepsilon}, \tag{24}$$

or in dimensionless form by defining a dimensionless surface charge density, $\bar{\sigma}_w$,

$$\frac{d\Phi}{dY}\bigg|_{Y=0} = -\bar{\sigma}_w = -\frac{h\sigma_w}{\varepsilon\zeta}. \tag{25}$$

Considering the potential at the wall to be zeta potential (i.e., $\Phi|_{Y=0} = 1$) and after substitution of Eq. (25) by Eq. (21), we have

$$n_h = \frac{\beta^2 \bar{\sigma}_w^2}{\kappa^2 h^2(e^{|\beta|(1-\Phi_h)} - 1)}. \tag{26}$$

Φ_h can be obtained by substituting the boundary condition, Eq. (15), into the solution of potential distribution, Eq. (22),

$$\Phi_h = 1 + \frac{2}{|\beta|}\ln(\cos\Omega). \tag{27}$$

Substituting Eq. (26) into Eq. (27), Φ_h is expressed in terms of $\bar{\sigma}_w$ as

$$e^{-(|\beta|(1-\Phi_h)/2)} = \cos\left(\frac{|\beta|\bar{\sigma}_w}{2\sqrt{(e^{|\beta|(1-\Phi_h)}-1)}}\right). \tag{28}$$

n_h and Φ_h are functions of surface charge density on the channel wall.

In this study, we assumed that the surface charge density only depends on the properties of the electrolyte and surface, and it does not change with the channel size and along the flow direction. This assumption is valid when channel width is larger than 10% of the Debye length. Therefore, the surface charge density on the wall is the same as the one on the wall in a semi-infinite medium ($h \to \infty$). The surface charge density can be related to zeta potential of the wall in a semi-infinite medium by solving the Poisson–Boltzmann equation.[20–22] The potential distribution is described by the nonlinear solution of the Poisson–Boltzmann equation for one-dimensional 1:1 electrolyte,

$$\psi = -\frac{2\zeta}{\beta}\ln\frac{e^{\kappa y}-\tanh(\beta/4)}{e^{\kappa y}+\tanh(\beta/4)}. \tag{29}$$

The surface charge density can be linked to the zeta potential by using Eqs. (24) and (29),

$$\sigma_w = -\varepsilon\left.\frac{d\psi}{dy}\right|_{y=0} = \frac{4\kappa\varepsilon\zeta}{\beta}\cdot\frac{\tanh(\beta/4)}{\tanh^2(\beta/4)-1}. \tag{30}$$

Equation (30) shows that the surface charge density depends on the permittivity of the electrolyte and the zeta potential of the channel wall. Therefore, specifying a value for the surface charge density or specifying a value for the zeta potential is equivalent, and one can be calculated if the other is given. For convenience of comparisons with others, the zeta potential of the wall is specified below.

By substituting Eq. (30) into Eqs. (26) and (28), n_h and Φ_h can be expressed in terms of zeta potential of the wall in a semi-infinite medium, respectively. The potential distribution inside the channel, defined by Eq. (22), can be determined. For the calculation of electric conductivity, the solution for charge density is also obtained from Eqs. (4), (7), and (22) as

$$\rho_e = \pm n_0 z e n_h \sec^2[\Omega(1-Y)], \tag{31}$$

where + for $\zeta < 0$ and − for $\zeta > 0$ and

$$\Omega = \frac{\kappa h\sqrt{n_h}}{2} = \frac{|\beta|\bar{\sigma}_w}{2\sqrt{e^{|\beta|(1-\Phi_h)}-1}}. \tag{32}$$

In the charge density profile described by Eq. (31), the contribution of coions has been ignored.

B. Average electric conductivity

With the solutions of electric potential and charge density distribution in the channel, we can calculate the average electric conductivity of the solution in the channel, which is essential for the calculation of electric field buildup, or streaming potential, along the flow direction. The electric conductivity λ of an electrolyte is a summation of contributions from all ions,[15,13]

$$\lambda = \sum^i \frac{z_i^2 e^2 A D_i n_i}{RT}, \tag{33}$$

where z_i is the valence of ith ion, A is Avogadro's number, D_i is the diffusion coefficient, and R is the universal gas constant. The average electric conductivity across the channel is defined as

$$\lambda_{av} = \frac{1}{h} \int_0^h \lambda \, dy. \tag{34}$$

For pure water, we only have to consider hydronium and hydroxyl ions,

$$\lambda_{av} = \frac{\lambda_0}{2h} \int_0^h (n_+ + n_-) \, dy, \tag{35}$$

where $\lambda_0 = 2z^2 e^2 A D n_0 / RT$ is the bulk electric conductivity of water with the assumption of $D_+ = D_- = D$. Here we define the bulk electric conductivity to be the electric conductivity of water with no influence of EDL. The diffusion coefficients for hydronium and hydroxyl are 9.31×10^{-9} and 5.28×10^{-9} m^2/s, respectively. The approximation of $D = 7.28 \times 10^{-9}$ m^2/s made the comparisons of the current model to other models easier without sacrificing the nature of the results. In a condition of strongly overlapped EDL, the diffusion coefficient should be closer to that of hydronium, 9.31×10^{-9} m^2/s, which could increase the average electric conductivity up to 25%. Therefore, the results based on an average diffusion coefficient of 7.28×10^{-9} m^2/s would show the effect of EDL overlapping based on a conservative estimation.

Using the solutions for ionic concentrations [Eq. (7)] and the potential distribution [Eq. (22)], the average conductivity across the channel can be obtained,

$$\lambda_{av} = \frac{\lambda_0}{2\Omega} \left[n_h \tanh(\Omega) + \frac{1}{n_h} \left(\frac{\sin 2\Omega}{4} + \frac{\Omega}{2} \right) \right]. \tag{36}$$

When the low concentration of coions is neglected, which is appropriate for strongly overlapped EDL, the average electric conductivity can be further simplified as

$$\lambda_{av} \approx \lambda_0 \frac{|\beta| \bar{\sigma}_W}{\kappa^2 h^2} = \lambda_0 \frac{|\sigma_W|}{2 n_0 z e h}. \tag{37}$$

Equation (37) shows that for strongly overlapped EDL, the average electric conductivity of the electrolyte is proportional to the bulk electric conductivity and the surface charge on the channel wall and is inversely proportional to channel width. The average electric conductivity is equal to the bulk electric conductivity when the channel width is infinitely large because $\Omega \to 0$ and $n_h \to 1$ as $h \to \infty$ as shown by Eq. (36).

In general, the total electric conduction along the microchannel consists of the surface conduction and fluid conduction. The surface conductivity depends on the material property of the microchannel. The fluid conductivity of the monovalent symmetric electrolyte under overlapped EDL condition is always much greater than the surface conductivity of the channel made of inorganic or polymeric materials.[1,23,24] For example, the glass made of borosilicate material has a surface conductivity of about 10^{-2} μS.[25,26] Therefore, the surface conduction was neglected in the calculation.

C. Pressure-driven flow inside the microchannel

For the flow inside the microchannel, the one-dimensional Navier–Stokes equation with Lorentz force adequately describes the momentum conservation,

$$\mu \frac{d^2 u}{dy^2} = \frac{dp}{dx} + \rho_e E_x, \tag{38}$$

where μ is the viscosity, u is the axial velocity, p is the pressure, and E_x is the electric field strength in axial direction, which can be expressed as the gradient of the axial potential, φ,

$$E_x = -\frac{d\varphi}{dx}. \tag{39}$$

The boundary conditions at the wall for the flow are

$$u = 0 \quad \text{at} \quad y = 0 \tag{40}$$

and

$$\frac{du}{dy} = 0 \quad \text{at} \quad y = h. \tag{41}$$

The velocity distribution along the y-direction can be solved from Eq. (38) with boundary conditions,

$$u = \frac{1}{\mu}\frac{dp}{dx}\left(\frac{y^2}{2} - hy\right) - \frac{\varepsilon E_x}{\mu}(\zeta - \psi), \tag{42}$$

or in dimensionless form,

$$\frac{U}{\text{Re}\dfrac{dP}{dX}} = \frac{Y^2}{2} - Y - \frac{\varepsilon\zeta}{h^2}R_{EP}(1 - \Phi), \tag{43}$$

where $U = u/u_{\text{ref}}$, $P = p/\rho u_{\text{ref}}^2$, $X = x/h$, Reynolds number $\text{Re} = \rho u_{\text{ref}} h/\mu$, u_{ref} is the average velocity of the cross-section, ρ is the density of water, and the ratio of electric field strength to the pressure gradient is defined as

$$R_{EP} = \frac{E_x}{dp/dx}. \tag{44}$$

In pressure-driven flow, the electric field strength E_x induced by the net charge moving downstream to generate a streaming potential can be calculated from the balance of electric current integrated over the cross-section of the channel I,

$$I = \int_0^h \rho_e u\,dy + h\lambda_{\text{av}}E_x = 0. \tag{45}$$

Combining Eqs. (23), (42), and (45), the solution for R_{EP} can be derived,

$$R_{EP} = \frac{-h^2 A}{\dfrac{\lambda_{\text{av}}\mu}{n_0 zen_h} + \varepsilon\zeta B}, \tag{46}$$

where A and B are the integration constants, which can be integrated and approximated as

$$A = \int_0^1 [\tan^2\Omega(1 - Y) + 1]\left(\frac{Y^2}{2} - Y\right)dY \approx 2.938\ln\frac{1.01\Omega^{-0.25} + 1.44}{0.002\Omega^{13} + 3} + \frac{1}{6} \tag{47}$$

and

$$B = \int_0^1 [\tan^2\Omega(1 - Y) + 1](\Phi - 1)dY \approx \frac{0.09}{|\beta|}e^{2.18\Omega^2 + 3\times10^{-4}\Omega^{20}} + (\Phi_h - 1)\frac{\tan\Omega}{\Omega}. \tag{48}$$

Equation (45) shows that the electric field strength caused by the streaming potential is proportional to the inverse of electric conductivity. Due to the increase in ionic concentration in overlapped EDL, the average electric conductivity is greater than without EDL overlap or the bulk

TABLE I. Properties of DIFU water.

Name	Symbol	Value	Unit
Ionic concentration (bulk)	n_0	6.02×10^{19}	$1/m^3$
Permeability	ε	7.08×10^{-10}	C/(V m)
Diffusivity	D	7.28×10^{-9}	m^2/s
Zeta potential	ζ	-0.086	V
Conductivity (bulk value)	λ_0	5.42×10^{-6}	S/m
Viscosity	μ	9.8×10^{-4}	kg/(m s)

value without the consideration of the EDL. As a result, the electric field strength is smaller than that obtained without the effect of EDL and overlapping EDL on the electric conductivity.

III. RESULTS AND DISCUSSION

Three cases were calculated for comparison: (1) a direct numerical solution of the Eqs. (1), (5), and (38), (2) an analytic solution of Eq. (20), which is based on approximation in Eq. (17), and (3) the solution of the Poisson–Boltzmann equation, which approximates the center of the channel having a condition of bulk water without any effect of the EDL. In this study, DIUF water is used as the electrolyte, and Table I shows the property of DIUF water at 300 K. The diffusion coefficients of hydronium and hydroxyl were approximated to be equal, as discussed earlier. The calculations compared the current overlapping EDL model to the semi-infinite model, the numerical solution of the Poisson equation, and the Nernst equation without any simplification under the same boundary conditions. For the numerical calculation, a solver in FLUENT software was used to solve user-defined differential equations. The number of grid points in the y-direction was chosen to be 164 to be grid-size independent.

The comparison of electric potential distribution in a cross-section of the channel is shown in Fig. 2 for three channel widths. The effect of overlapping EDL from the two channel walls is apparent as the curves change with κh. The potential distribution shows high potential at the wall
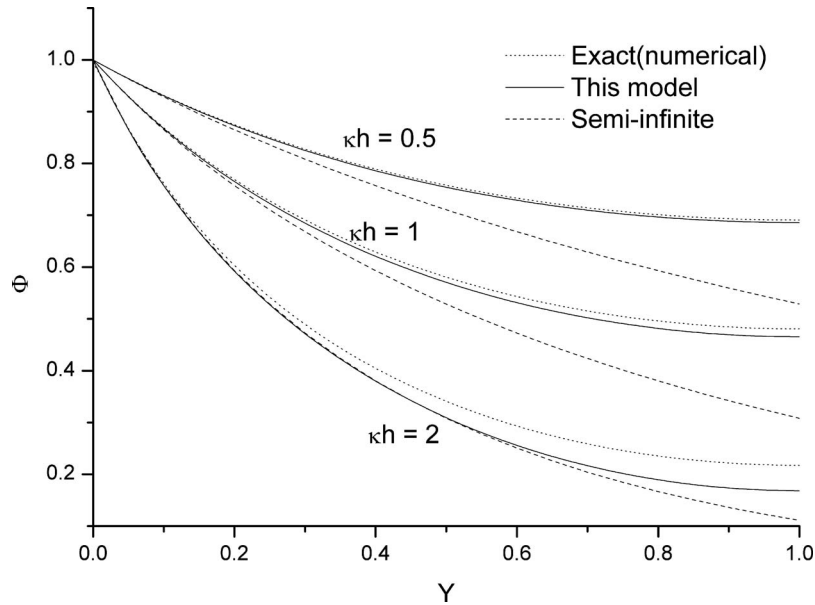

FIG. 2. Dimensionless potential distribution in the cross-section of the microchannel. The dimensionless potential and dimensionless channel width are defined by Eqs. (9) and (10), and a decreasing κh (the ratio of channel half width to the Debye length) represents increased EDL overlap.
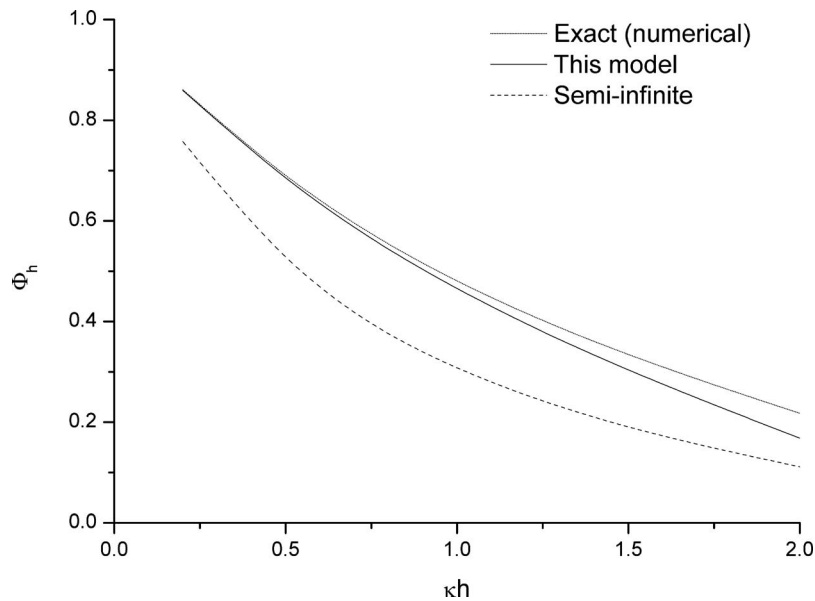
FIG. 3. Dimensionless potential at the center of the microchannel at different ratios of channel half width to the Debye length. The exact solution was obtained numerically with no approximations, and the current analytic model neglected the contribution of coions. The semi-infinite model assumed the center of the channel having the condition of bulk water without any effect of EDL overlap.

and low potential at the center of the channel. The solution of the semi-infinite model does not have a zero gradient of potential distribution at the channel center, while the current model uses the symmetric condition at the channel center (zero potential gradient). The current model is clearly better and closer to the exact solution in all three cases, and it is closer to the exact solution as the channel narrows. When the channel width is equal to or less than the Debye length, the result of the current model is almost identical to the exact solution. The electric potential at the center of the channel, at various channel widths, is shown in Fig. 3. As expected the current model is shown to be better than the semi-infinite model and closer to the exact solution. The narrower the channel, the closer the solution of the current model to the exact solution.

Using the solution of surface charge [Eq. (30)], the average conductivity of DIUF water under the condition of overlapping EDL was obtained and shown in Fig. 4 for three levels of surface zeta potential. The average electric conductivity across the microchannel width is significantly greater than the bulk electric conductivity value for all three zeta potential levels. This is caused by the increased ionic concentration in the EDL because the increase in the average electric conductivity is greater when the channel is narrower. Higher zeta potential of the surface also results in a greater increase in the average electric conductivity. The magnitude of the increase ranges from 10 to 100, as shown in Fig. 4.

Figure 5 shows the effect of the EDL on the velocity distribution across the microchannel width when $\kappa h = 0.5$. Compared to the channel flow without the influence of the EDL, the existence of the EDL reduces the flow rate about 4.1% under the same pressure gradient. If electric conductivity is the same as the bulk value λ_0, the velocity decrease would be 25.8%.

The ratio of pressure drop calculated using the current electric conductivity model and using the bulk electric conductivity value to the pressure drop calculated without EDL effect, $\Delta p_{EDL} / \Delta p_{no\ EDL}$, is shown in Fig. 6. When the EDL is considered, the pressure drop is always greater than that without the EDL. In other words, the EDL will increase the pressure drop in a pressure-driven flow. However, the current model predicts a smaller increase in pressure drop due to the increased value of the electric conductivity. The effect of the EDL in the current model is larger when the channel width is larger ($0.1 \leq \kappa h \leq 2$). When $\kappa h > 2$, the current model is no longer applicable due to the narrow channel approximation ($\kappa h \leq 2$). Because the constant surface
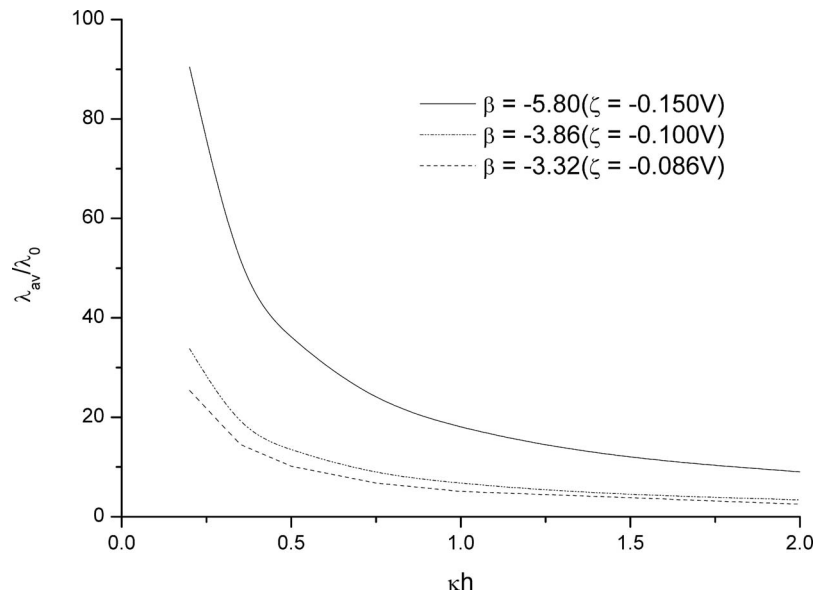
FIG. 4. Average electric conductivity as a function of the ratio of channel half width to the Debye length under different surface zeta potentials.

charge is used in the current model, its application is limited to $\kappa h > 0.2$. As a comparison, the increase in pressure drop from the model using the bulk electric conductivity, without considering the influence of ionic concentration on the electric conductivity, rises to a maximum at $\kappa h = 0.75$. The existence of the maximum in pressure drop has also been suggested by others in the investigation of the EDL effect on apparent viscosity of fluid in charged capillaries.[6] Bharti found that electroviscous effect decreased monotonically as κh increased and attributed the effect to the constant surface change condition used in their calculation. It was also pointed out that the
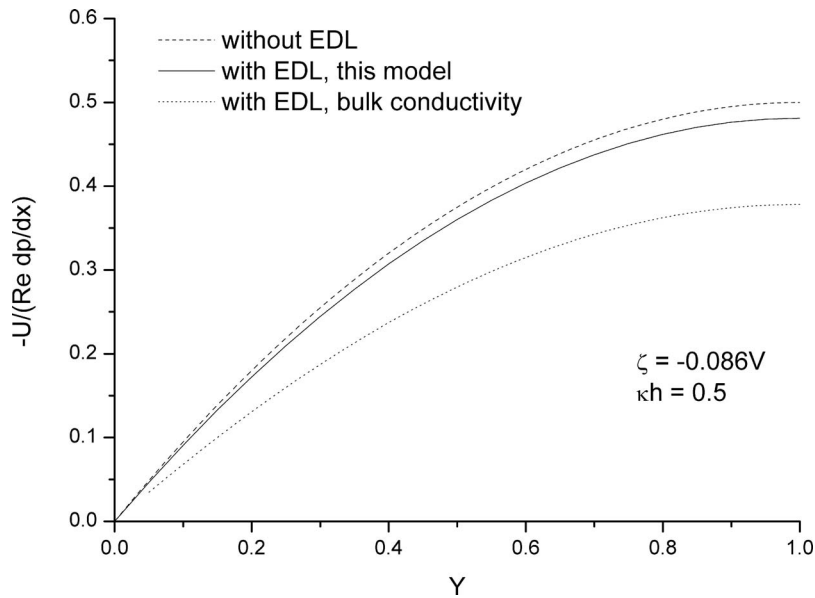

FIG. 5. Velocity distributions across the channel using two different electric conductivity values: bulk water conductivity and the average conductivity accounting EDL overlap. Water velocity distribution without considering EDL effect is also shown as the basis for comparison.
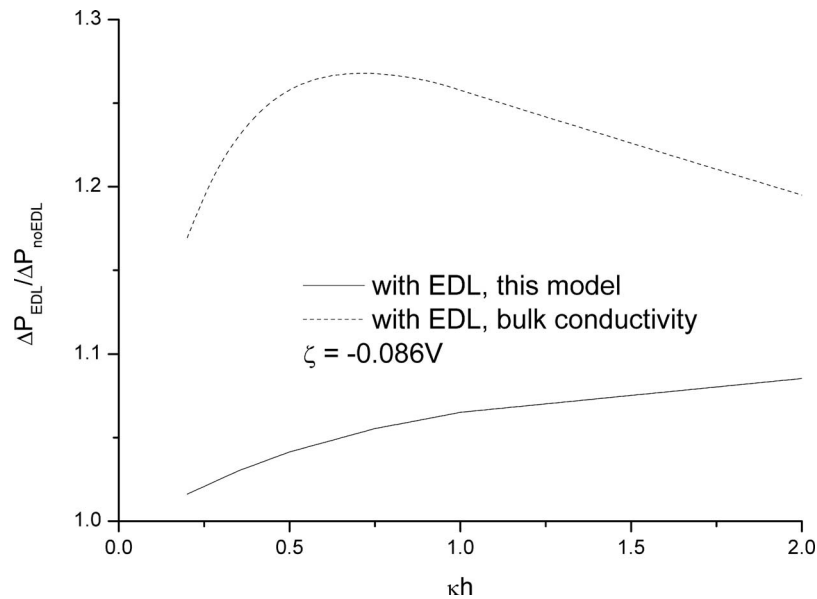
FIG. 6. Ratio of pressure drop calculated using the current electric conductivity model and using the electric conductivity of bulk water to the pressure drop calculated without EDL effect.

calculation based on a constant surface potential would lead to the occurrence of a local maximum as κh varies.[17] Although neither constant surface charge nor constant surface potential is true when EDL on two walls overlaps, the current model indicates that if the electric conductivity does not include the effect of increased ion concentration inside the EDL for narrow channels, the effect of the EDL on pressure drop in pressure-driven flows may be overestimated.

IV. CONCLUSION

In this study, the Poisson equation, Nernst equation, Navier–Stokes equation, and the electric current continuity equation are solved with overlapping EDL for a channel with a width around Debye length ($\kappa h = 0.2 \sim 2$). The results are compared with the numerical exact solution and the semi-infinite model. The conclusions include the following.

(1) The current model for the potential distribution in the microchannel, which includes the effect of overlapping EDL, produces better results (i.e., closer to exact solution) than the results calculated by models using Poisson–Boltzmann distribution for a semi-infinite medium. For all cases, when the channel width is about Debye length ($0.2 < \kappa h < 2$), the current model can be used to determine the effect of overlapping EDL. When the channel width decreases, the current model is much closer to the exact solution.

(2) Because the counterion concentration inside the EDL is significantly larger, the resulting average electric conductivity across the channel is much greater than the bulk electrolyte electric conductivity. The increase in the average electric conductivity is much greater as the channel width decreases, and the range of such increase is 10–100 times the bulk electrolyte electric conductivity ($0.2 < \kappa h < 2$). The results indicate that the increase in the average conductivity of the electrolyte inside the channel results in a much smaller streaming potential.

(3) Compared to the flow without the EDL, the pressure drop inside the microchannel with overlapping EDL will increase (4.1% for $\kappa h = 0.5$, $\zeta = -0.086$ V). However, such increase is less than the prediction (25.8%) when the effect of the electric conductivity increase is neglected and the bulk electric conductivity of the electrolyte is used.

As an initial effort, this study used pure water without any salts or dissolved gases, which is

an idealized case, to show the effect of overlapped EDL on electric conductivity. Further studies could include salts and buffer solutions to produce results closer to practical applications.

[1] R. J. Hunter, *Zeta Potential in Colloid Science: Principles and Applications* (Academic, New York, 1981).
[2] P. C. Hiemenz and R. Rajagopalan, *Principles of Colloid and Surface Chemistry*, 3rd ed. (Dekker, New York, 1997).
[3] R. J. Yang, L. M. Fu, and C. C. Hwang, J. Colloid Interface Sci. **244**, 173 (2001).
[4] G. E. Karniadakis and A. Beskok, *Micro Flows Fundamentals and Simulation* (Springer-Verlag, New York, 2002).
[5] F. Tian and D. Y. Kwok, Langmuir **21**, 2192 (2005).
[6] W. R. Bowen and F. Jenner, J. Colloid Interface Sci. **173**, 388 (1995).
[7] W. Qu and D. Li, J. Colloid Interface Sci. **224**, 397 (2000).
[8] D. Li, Colloids Surf., A **195**, 35 (2001).
[9] M.-S. Chun and H. W. Kwak, Korea-Aust. Rheol. J. **15**, 83 (2003).
[10] D. Burgreen and F. R. Nakache, J. Phys. Chem. **68**, 1084 (1964).
[11] C. L. Rice and R. Whitehead, J. Phys. Chem. **69**, 4017 (1965).
[12] S. Levine, J. R. Marriott, G. Neale, and N. Epstein, J. Colloid Interface Sci. **52**, 136 (1975).
[13] J. M. MacInnes, Chem. Eng. Sci. **57**, 4539 (2002).
[14] J. Yang, J. H. Masliyah, and D. Y. Kwok, Langmuir **20**, 3863 (2004).
[15] F. Lu, J. Yang, and D. Y. Kwok, J. Phys. Chem. B **108**, 14970 (2004).
[16] M. R. Davidson and D. J. E. Harvie, Chem. Eng. Sci. **62**, 4229 (2007).
[17] R. P. Bharti, D. J. E. Harvie, and M. R. Davidson, Chem. Eng. Sci. **63**, 3593 (2008).
[18] C. L. Ren and D. Li, Anal. Chim. Acta **531**, 15 (2005).
[19] T. W. Healy and L. R. White, Adv. Colloid Interface Sci. **9**, 303 (1978).
[20] R. J. Hunter, *Foundations of Colloid Science*, 2nd ed. (Oxford University Press, New York, 2001).
[21] F. Andrietti, A. Peres, and R. Pezzotta, Biophys. J. **16**, 1121 (1976).
[22] W. K. Chandler, A. L. Hodgkin, and H. Meves, J. Physiol. (London) **180**, 821 (1965).
[23] M.-S. Chun, T. S. Lee, and N. W. Choi, J. Micromech. Mecroeng. **15**, 710 (2005).
[24] M.-S. Chun, S.-Y. Lee, and S.-M. Yang, J. Colloid Interface Sci. **266**, 120 (2003).
[25] L. Ren, D. Li, and W. Qu, J. Colloid Interface Sci. **233**, 12 (2001).
[26] C. Werner, H. Korber, R. Zimmermann, S. Dukhin, and H.-J. Jacobasch, J. Colloid Interface Sci. **208**, 329 (1998).